Published in final edited form as:
Angew Chem Int Ed Engl. 2008 ; 47(40): 7592–7601. doi:10.1002/anie.200800918.

Bifurcations on Potential Energy Surfaces of Organic Reactions

Daniel H. Ess, **Steven E. Wheeler**, **Robert G. Iafe**, **Lai Xu**, **Nihan Çelebi-Ölçüm**, and **K. N. Houk [Prof.]***

Abstract

A single transition state may lead to multiple intermediates or products if there is a post-transition state reaction path bifurcation. These bifurcations arise when there are sequential transition states with no intervening energy minimum. For such systems, the shape of the potential energy surface and dynamic effects control selectivity rather than transition state energetics. This minireview covers recent investigations of organic reactions exhibiting reaction pathway bifurcations. Such phenomena are surprisingly general and affect experimental observables such as kinetic isotope effects and product distributions.

Keywords

Valley-ridge Inflection; Two-Step No Intermediate; Bis-pericyclic; Quantum Mechanical Calculations

1. Introduction

A transition state is the highest energy point along the minimum energy path connecting reactants and products, usually connecting one set of reactants with one set of products. However, a single transition state can be shared by two or more reaction pathways if there is a post-transition state bifurcation. Bifurcations occur when there are sequential transition states with no intervening intermediate; such a surface involves a valley-ridge inflection (VRI),[1] where the potential energy surface (PES) valley changes into a dynamically unstable ridge (Figure 1).[2] This type of potential energy surface describes a reaction mechanism that is different from stepwise or concerted and has been referred to as a two-step no intermediate mechanism.[3] When a reaction has this type of surface, the rate of selective formation of one product relative to another is governed by the potential energy surface shape and resulting dynamic effects.[4]

Early examples found of bifurcating reactions involved simple isomerizations and rearrangements,[2] including, for example, the addition of HF to ethylene which can yield either of two equivalent rotamers of fluoroethane.[5] Recently, however, several complex organic reactions, most notably pericyclic reactions, have been shown to involve bifurcating reaction paths. This minireview covers recent examples of isomerizations, substitutions, and pericyclic reactions that involve reaction path bifurcations.

A stationary point on a molecular potential energy surface is a point in the 3N-6 dimensional configuration space where the energy gradients (forces) with respect to nuclear positions are all zero.[6] Characterization of a stationary point as either a minimum or saddle point requires the evaluation of second derivatives, or force constants. When all second derivatives are

*Department of Chemistry and Biochemistry, University of California, Los Angeles, 607 Charles E. Young Drive East, Los Angeles, CA 90095, (USA), (+ 1) 310-206-1843, E-mail: houk@chem.ucla.edu.

positive, the stationary point is a minimum, while one negative second derivative indicates a saddle point.[7] In typical quantum mechanical calculations, characterization of stationary points is achieved by diagonalizing the matrix of mass-weighted second derivatives (the Hessian) to yield normal vibrational modes (eigenvectors) and the associated force constants (eigenvalues).[6]

Along the floor of a downward sloping valley, one gradient is negative and all others are zero, with positive force constants. If two transition states occur sequentially with no intervening intermediate, the curvature of the energy surface along one direction perpendicular to the reaction coordinate must change from positive to negative; that is, the valley floor becomes a ridge at some point in this 2D configuration space. The point where this occurs is the valley-ridge inflection point. Here the Hessian has one zero eigenvalue corresponding to a motion perpendicular to the gradient.[7] Near the VRI, the single reaction pathway branches into two; there is no longer a restoring force for molecular motion perpendicular to the reaction coordinate. However, unlike minima and saddle points, the location of a valley-ridge inflection point is dependent upon the choice of coordinate systems.[8]

The intrinsic reaction coordinate (IRC) is the most common quantum mechanical reaction pathway description.[9] This is a mass-weighted steepest decent path, following the negative gradient downhill from a transition state. Physically, the IRC corresponds to the pathway travelled by nuclei moving on the PES with infinitesimal velocities and is typically considered the theoretical minimum energy pathway (MEP). However, when the gradient becomes zero or a potential energy surface is flat, a single IRC cannot describe a unique preferred reaction trajectory.[10]

Figure 1 shows the difference between an IRC pathway (dotted lines) and qualitative dynamic trajectories (white arrows) for a symmetrical model potential energy surface with two sequential transition states and an intervening valley-ridge inflection point. The IRC is the steepest descent pathway from **TS1** and follows the valley floor in this region. After passing through the valley-ridge inflection point, the IRC stays on the developing ridge before stopping at **TS2**. From **TS2**, the IRC exhibits the typical reaction path behavior, following the normal coordinate corresponding to the imaginary vibrational frequency, connecting the two products. Representative reaction trajectories that would result from dynamic simulations are depicted by the white arrows, and show that typical trajectories deviate from the IRC in the vicinity of the **VRI**, bypassing **TS2**.[11] Several groups are actively investigating alternative theoretical treatments of hypersurfaces to rigorously define a reaction pathway when a VRI occurs.[12] Methods include reaction path Hamiltonians,[13] reduced gradient following,[14] gradient extremals,[15] transition path sampling,[16] and the distinguished coordinate method.[17]

2. Unimolecular Isomerization Reactions

One of the most thoroughly studied reactions with a reaction pathway bifurcation is the isomerization of methoxy radical, **1** (Figure 2). *Ab initio*, DFT, and dynamic simulation studies all yield similar conclusions about the potential energy surface shape and mechanism of this rearrangement.[12,18–20] Figure 2 shows the potential energy hypersurface in terms of the C-O-H angle and one of the HCOH dihedral angles. The reaction first proceeds through a three membered C_s transition state for hydrogen migration (**2**). The reaction pathway bifurcates between TS **2** and TS **3** due to an intervening VRI. After the VRI, the OH group rotates in or out of the plane leading to either of the equivalent forms of **4**. TS **3**, corresponding to rotation about the C-O bond, arises from the OH bond eclipsing the half-filled hybridized methylene orbital.

Studies on the monodeuterated methoxy radical derivative, H_2DCO,[18] have provided insight into vibrational effects on the product ratio. In the all hydrogen case, the mass-weighted PES

is symmetrical, leading to equal reaction pathway branching toward two equivalent forms of **4**. However, for the deuterium substituted version, *ab initio* wave packet dynamic simulations have shown that the slight asymmetry induced by a deuterium atom creates a branching preference where the hydrogen atom is transferred *cis* to the deuterium atom on the now slightly unsymmetrical mass-weighted PES.[19]

The complete active space (CAS)-SCF potential energy surface for cyclooctatetraene (COT) bond shifting is shown in Figure 3.[21–23] Starting from one of the D_{2d} symmetric tub structures, there is a flat D_{4h} saddle point corresponding to tub inversion, with localized-alternating single and double bonds. This saddle point can be converted to an equivalent D_{4h}-symmetric structure by passing through the planar, antiaromatic D_{8h} saddle point. Alternatively, starting from this D_{8h}-symmetric saddle point, there are two bifurcating reaction pathways leading directly to four equivalent tub structures, bypassing the D_{4h} structures (see red lines). Features of this complex PES have been confirmed by a photodetachment study of the COT anion.[22]

There is also a bifurcation along the reaction pathway for the transformation of COT to semibullvalene (Scheme 1).[24] Instead of involving the bicyclo[3.3.0.0]octa-1,6-dien-4,8-diyl diradical (**5**) in a stepwise process, the CAS(MP2)/CASSCF PES computed by Castaño and co-workers suggests that this reaction first proceeds through the rate-determining TS **6**. The reaction path then branches between **6** and the Cope TS **7**, yielding either of the equivalent forms of semibullvalene

Other isomerization reaction pathways with bifurcations include the transformation of fulminic acid (HCNO) to isocyanic acid (HNCO),[25] ketene-ketenimine rearrangement,[26] and the photochemical formation of singlet carbene and N_2 from diazirine, where the bifurcation leads to two different S_0/S_1conical intersections.[27]

3. Substitution Reactions

Aldehyde anion radical addition to alkyl halides is hypothesized to occur either by electron-transfer (ET) or substitution mechanisms (Figure 4a). Shaik and co-workers have shown that these mechanisms actually involve a common TS and a PES bifurcation.[28] Figure 4b outlines the computed *ab initio* PES for the reaction of formaldehyde anion radical with methylchloride. After an initial van der Waals complex, there is an electron-transfer TS, **8**, immediately followed by the TS for radical addition, **9**. Because of a PES bifurcation, the mass-weighted IRC leads from **8** to the C-substitution product **10** (which was not the experimentally observed major product) whereas the steepest descent path in non-mass-weighted coordinates connects TS **8** to the electron transfer product **11**.

Schlegel *et al*.[29] and others[30] provided further insight into this system based on *ab initio* molecular dynamics simulations of formaldehyde and NCCHO radical anions with methyl chloride and fluoride. The predicted product distribution for the reaction in Figure 4b at 298 K was 54:12:12:22 for ET, C-substitution, O-substitution, and return to reactants, respectively. Schlegel *et al*. found that the branching ratio was roughly correlated with the C-C bond distance in the electron transfer transition state; long C-C distances in **8** lead to **11**, while short C-C distances lead to **10**.

4. Pericyclic Reactions

4.1 Electrocyclic reactions

One of the earliest identified examples of a PES bifurcation was reported by Valtazanos *et al*. for the ring opening of cyclopropylidene (**R**) to allene (**P1**/**P2**, Figure 5a).[2, 31] Their

computed MCSCF hypersurface, mapped with the coordinates for the average conrotatory angle (δ) and the ring opening C-C-C bond angle (ϕ), is shown in Figure 5b. In cyclopropylidene, the methylene groups are orthogonal to the ring plane (δ = 90°, ϕ = 55°). In the initial stages of the reaction, δ remains constant at 90° and only disrotatory motion (change in ϕ) occurs. The first of two sequential transition states involves C-C-C ring angle increase to 80° in combination with disrotatory movement of the methylene groups while maintaining C_s symmetry until the C-C bond is broken. As the ring angle increases further, the steepest decent path leads to the transition state that interconverts equivalent allene structures via methylene group rotation. The reaction pathway bifurcates near the VRI (located at ~δ = 90° and ϕ = 84°) then allowing conrotatory displacement to mix into the reaction pathway, breaking C_s symmetry.

Using B3LYP-DFT, Nouri and Tantillo found that the sigmatropic shift and electrocyclic ring opening steps for cyclopropylcarbinyl carbocation **12** occur sequentially with no intermediate.[32] On this PES, the shared TS is for the 1,2-hydride shift, followed by the disrotatory ring opening TS. The reaction pathway bifurcates, leading to allyl cation **13** or **14**.

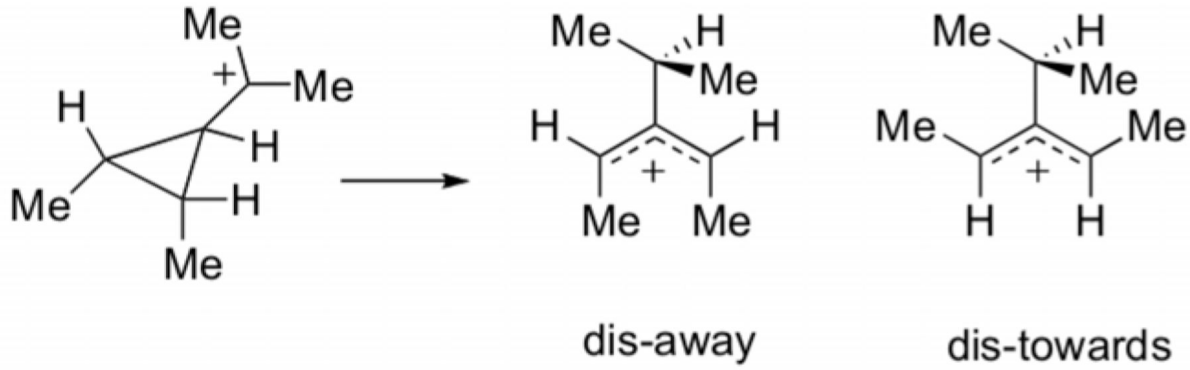

Birney and co-workers have reported an electrocyclic ring opening with an uphill PES bifurcation for the thermal deazetization reaction of heterocyclic nitrosimine **15** (Scheme 2).[33] The reaction proceeds by sequential TSs for C-N bond rotation (**16**) and pseudopericyclic cyclization (**18**), which then leads to N_2 loss via intermediate **19**. Interestingly, the analogous ring opening of oxetene gives only one concerted transition state, mixing ring opening and dihedral rotation motions simultaneously.

5.2 Sigmatropic Rearrangements

Hrovat, Duncan, and Borden investigated the Cope rearrangement of 1,2,6-heptatriene **20** (Figure 6).[34] Evidence of both stepwise and concerted mechanisms has been observed experimentally.[35] However Borden and co-workers only found a single concerted TS, **21**. Formation of either the concerted rearrangement product (**22**) or the diradical intermediate (**24**) was predicted, depending on whether an IRC was computed using DFT or CASSCF methods. Dynamics simulations using a reparameterized semiempirical MO model (AM1-SRP) fit to CASSCF stationary points showed that 17% of the trajectories follow a “concerted” pathway.[36]

Houk and co-workers have identified a similar type of bifurcation on the PES for the [3,3] rearrangement of 6-methylenebicyclo[6.2.0]hep-2-ene, which yields a diradical intermediate or 5-methylenenorbornene.[37]

Bifurcations also exist on the PESs for the rearrangements of *cis*-bicyclo[6.1.0]nona-2,4,6-triene, 9,9-dicyanobicyclo[6.1.0]nona-2,4,6-triene,[38] *cis*-1,2-divinylcyclobutane, and

cis-1,2-divinylcyclo-propane.[39] In these reactions, the C_s-symmetric Cope TS is followed by the C_s boat interconversion TS with no intervening intermediate. In each case, the result is a bifurcating reaction pathway that leads to either of two equivalent boat structures.

5.3 Ene Reactions

The mechanism of the singlet oxygen ene reaction has been studied extensively.[40] Three mechanisms—concerted, stepwise, and exciplex perepoxide formation—have all been proposed based on experimental and theoretical considerations (Scheme 3). Early *ab initio* studies favored stepwise mechanisms,[41] while measured kinetic isotope effects (KIEs) and observed stereospecific suprafacial product formation suggest a concerted mechanism or perepoxide mechanism.[42]

A collaborative effort by the Singleton, Houk and Foote groups used ^{13}C KIEs and quantum mechanical methods to show that this reaction takes place via a two-step no intermediate mechanism.[3,43] CCSD(T) single point energies computed on a grid of B3LYP structures revealed that the PES bifurcates after a common TS, **26**, (Figure 7). The second sequential TS, **27**, is the "elusive" perepoxide-like structure with shorter partial C-O bond lengths, and connects the two ene-products. When branching occurs on this surface, the C-H bond breaks and O-H bond forms. Quasiclassical dynamic simulations on a B3LYP surface[44] predicted $k_H/k_D = 1.38$, close to the experimental value of ~1.4. The origin of this isotope effect is different than typical isotope effects, which arise from differences in transition state zero-point energies. In this case the effect arises due to changes in the curvature of the mass-weighted PES, which in turn lead to different dynamics trajectories between the H and D substituted cases. The value of 1.4 is related to the $\sqrt{2}$ ratio of stretching frequencies of the CH and CD bonds broken in the reaction. Lluch and co-workers located the VRI at a C-O bond length of 1.90 for O_2 addition to (deuterated)tetramethylethylene.[45]

The ene reaction of allene **29** forms the C^2-C^6 cyclization product **30** (Figure 8).[46,47] Singleton and co-workers have shown that there is a single concerted-like TS (**31**) that leads to either the diradical intermediate **32** or the concerted ene product (**30**). Figure 8 shows Singleton's qualitative unsymmetrical bifurcating surface and B3LYP stationary points. Because the sequential transition states are offset, the MEP/IRC connects TS **31** to **30**. However, possible trajectories can pass over **31** and go to the diradical intermediate (**32**). The amount of **32** formed will depend on the exact shape of the surface. Quasiclassical dynamics simulations on a B3LYP surface showed that 29 out of 101 trajectories deviate from the MEP and form the diradical intermediate. This is consistent with experimentally trapped diradical intermediates and the measured KIE (~1.4, again), which is too large for a stepwise mechanism but too small for concerted. Schmittel and co-workers have recently confirmed this bifurcation model experimentally by observing large differences in intermolecular and intramolecular KIEs for several substituted versions of **29**.[48]

5.4 Cycloadditions

Both Sakai and Nguyen[49] and Cremer and co-workers[50] have described the bifurcation on the PES for the concerted cycloaddition of *cis*-1,3-butadiene with ethylene. After the C_s Diels-Alder TS the reaction path bifurcates, leading to either of the half-chair cyclohexenes.

Caramella *et al*.[51–54] brought the role of bifurcations to the attention of many chemists through the remarkable finding that some of the simplest Diels-Alder reactions involve surface bifurcations. In a series of landmark papers, Caramella and co-workers showed that several endo diene dimerizations, such as methacrolein,[51] cyclopentadiene, [52] butadiene, [53] and cyclopentadieneone[54] occur along bifurcating reaction paths. Previously, diene dimerization reaction selectivity was viewed as the result of competing TSs. Figure 9a shows a model

contour plot of a PES with two competing cycloaddition transition states, **TSa** and **TSb**, a second-order saddle point (**SOSP**) that connects them, and the Cope TS (**TSc**), corresponding to isomerization of the cycloadducts. In the diene dimerizations studied by Caramella and others,[55] **TSa** and **TSb** have merged into a single "bis-pericyclic" transition state, **TS1** (Figure 9b). On such a surface, the second-order saddle point is lost and a VRI point intervenes between the bis-pericyclic TS and the Cope TS, **TS2**.

While there are two possible [4 + 2] cycloaddition pathways for cyclopentadiene dimerization (Scheme 4a), a single highly asynchronous Diels-Alder transition state, (**34**, Scheme 4b) is found. The primary [2 + 4] interactions are equal in magnitude to the [4 + 2] interactions, resulting in one short partial bond (1.96 Å) that is common to both interactions, and two equivalent long partial bonds (2.90Å). The IRC leads directly from **34** to the Cope TS (**35**), with only a slight decrease in energy (2.3 kcal/mol) and shortening of all three bonds. The two endo cycloaddition pathways have merged at the bis-pericyclic TS and split at a VRI in between **34** and **35**, leading to one of two equivalent endo cycloadducts. Lasorne and co-workers located the valley-ridge inflection structure with partial bond lengths of 1.87 Å and 2.87 Å.[56]

Houk and co-workers have studied a series of tethered (intramolecular) cyclobutadiene-butadiene cycloaddition reactions with bifurcating PESs.[57] Figure 10 shows the influence of the tether length on the shape and branching ratios (white arrows) for trimethylene and tetramethylene tethers. The Diels-Alder and Cope TSs are nearly aligned relative to each other along the reaction coordinate in the trimethylene tether case, and are predicted to give roughly equal ratios of [2 + 2] and [4 + 2] cycloadducts. The longer tetramethylene tether substantially offsets the positions of these transition states, resulting in a highly unsymmetrical surface with a large preference for formation of the [4 + 2] cycloadduct.

More recently, our group has found that periselectivity for cycloadditions of cyclopentadiene with nitroalkenes and α-keto-β,γ-unsaturated phosphonates under thermal and Lewis-acid catalyzed conditions are controlled by a bis-pericyclic TS.[58] Under thermal conditions, cyclopentadiene acts as the 4π-diene component in the cycloaddition with nitroethylene (**36**) and the Diels-Alder (DA) adduct, **37**, is the major product (Scheme 5). Selectivity is reversed with Lewis acid, $SnCl_4$, and the hetero-Diels-Alder (HDA) adduct (**38**) is preferred. Figure 11 shows a qualitative comparison of the thermal and Lewis-acid catalyzed bifurcating PESs with geometries of the bis-pericyclic Diels-Alder TSs (**TS1**) above and the Claisen TSs (**TS2**) below each surface. Preference for the Diels-Alder adduct under thermal conditions is due to the shorter C-C bond compared to the C-O interaction. $SnCl_4$ coordination decreases the C-O bond length and increases the C-C distance leading to a preference for C-O bond formation along the IRC. Effectively, $SnCl_4$ skews the bis-pericyclic TS toward the hetero-Diels-Alder adduct, and now only trajectories deviating significantly from the MEP lead to the Diels-Alder adduct.

Singleton and co-workers showed that the cycloaddition of cyclopentadiene with diphenylketene affords Diels-Alder and hetero-Diels-Alder cycloadducts from a bis-pericyclic TS.[59] It is likely that bis-pericyclic TS geometries are good predictors of periselectivity, but there is no simple way to quantitatively predict branching ratios without dynamics simulations.

Bis-pericyclic TSs are also involved in complex cycloaddition reactions used in natural product synthesis. For example, Quideau and co-workers have shown that a bis-pericyclic Diels-Alder transition state controls diastereofacial selectivity in the dimerization of orthoquinols for the synthesis of (+)-Aquaticol, a bis-sesquiterpene.[60] Cycloaddition bifurcations were also reported for the reaction of 1,2,4,5-tetrazines and pyridazines with alkynes, the cycloaddition of cycloheptatriene and cyclopentadiene,[61] 1,3-dipolar cycloadditions,[62] and dichlorocarbene addition to cyclopropene.[63]

Conclusions and Outlook

The possibility that multiple intermediates and/or products can be formed from a single transition state expands the scope of possible reaction pathways and complicates classic distinctions between stepwise and concerted mechanisms. Lluch and co-workers have proposed the use of variational transition state theory to predict product distributions in the case of symmetric bifurcating reaction pathways made unsymmetric by isotopic substitution.[45] However, in general, when a PES bifurcation occurs, analysis of the entire potential energy surface is critical for a qualitative understanding of reaction pathways. Presently, molecular dynamics simulations are often necessary to give quantitative predictions of selectivity and isotope effects for these cases, since product distributions are no longer dictated by relative free energies of competing transition states.[59] Bifurcation theory impacts many physical observables such as kinetic isotope effects and product ratios.

The last decade has witnessed a flurry of reports of reaction path bifurcations in organic reactions, precipitated in part by the pioneering work of Caramella *et al*. on bis-pericyclic reactions.[51–54] Future work will undoubtedly uncover many more examples of post-transition state reaction path bifurcations in pericyclic reactions. The sundry examples described in this review demonstrate that reaction path bifurcations are not mere curiosities, but may be quite general for many types of organic and organometallic transformations.[64]

Biographies

Daniel H. Ess completed his undergraduate studies at Brigham Young University and then spent two years as a full-time volunteer for the Church of Jesus Christ of Latter-day Saints. He completed his Ph.D. under the direction of K. N. Houk and is currently a post-doctoral scholar at California Institute of Technology with William A. Goddard III and at The Scripps Research Institute in Florida with Roy A. Periana.

Steven E. Wheeler was born in Richmond, Virginia. He graduated from New College of Florida with a B.A. in Chemistry and Physics. He completed his Ph.D. in Fritz Schaefer's group at the University of Georgia before joining the Houk group as a postdoc in 2006. He is currently a NIH NRSA postdoctoral fellow, studying the prediction of catalytic proficiencies of enzymes, enzyme design, and π-stacking interactions.

Robert G. Iafe was born in San Diego, California in 1982. He graduated with Honors in 2004 from Loyola Marymount University with a B.S. in Chemistry. He completed his M.S. in Ken Houk's group at UCLA. He is currently pursuing his Ph.D. in chemistry, studying pericyclic reaction mechanisms and C-H activation using transition metals under the supervision of Ken Houk and palladium mediated coupling reactions with Craig Merlic.

Lai Xu was born in Lanzhou, China in 1983. She graduated in 2005 from Peking University in China with a BS in chemistry. She is currently a graduate student in the Houk group at UCLA, studying dynamics of 1,3-dipolar cycloaddition reactions.

Nihan Çelebi-Ölçüm received her B.S. degree from Boğaziçi University (Istanbul, Turkey) in 1997 and her M.S. degree in Computational and Theoretical Chemistry from Université Henri Poincaré (Nancy, France) in 1999. She then worked for Nevzat Pharmaceuticals, Analytical R&D Department (Istanbul) until 2004. She is currently a Ph.D. student under the direction of Prof. V. Aviyente at Boğaziçi University and has been a visiting graduate student at UCLA.

K. N. Houk was an undergraduate and graduate student at Harvard, working with R. B. Woodward. He has been on the faculties of LSU, the University of Pittsburgh, and UCLA. He received the American Chemical Society James Flack Norris Award in Physical Organic Chemistry and the Award for Computers in Chemical and Pharmaceutical Research. His group is involved with the exploration of organic and biological reactions with computational methods.

Acknowledgments

We are grateful to the National Science Foundation for financial support (CHE-0548209) and a traineeship to DHE [NSF IGERT: Materials Creation Training Program (DGE-0114443)]. SEW is supported by a NIH NRSA postdoctoral fellowship (NIH-1F32GM082114-01), while NÇ-Ö is supported by the Scientific and Technological Research Council of Turkey (TÜBİTAK).

References

1. Carpenter, BK. Reactive Intermediates Chemistry. Moss, RA.; Platz, MS.; Jones, M., Jr, editors. Hoboken, NJ: Wiley-Interscience; 2004.
2. Valtazanos P, Ruedenberg K. Theor. Chim. Acta 1986;69:281.
3. Singleton DA, Hang C, Szymanski MJ, Meyer MP, Leach AG, Kuwata KT, Chen JS, Greer A, Foote CS, Houk KN. J. Am. Chem. Soc 2003;125:1319. [PubMed: 12553834]
4. Hamaguchi M, Nakaishi M, Nagai T, Nakamura T, Abe M. J. Am. Chem. Soc 2007;129:12981. [PubMed: 17924620]
5. Minyaev RM, Wales DJ. Chem. Phys. Lett 1994;218:413.

6. Fueno, T. The Transition State. Tokyo: Gordon and Breach Science; 1999.
7. Kraka, E. Encyclopedia of Computational Chemistry. Schleyer, PvR, editor. Vol. Vol. 4. New York: Wiley; 1998. p. 2445
8. Wales DJ. J. Chem. Phys 2000;113:3926.
9. Fukui K. Acc. Chem. Res 1981;14:363.
10. Carpenter BK. Acc. Chem. Res 1992;25:520.Doubleday C, Nendel M, Houk KN, Thweatt D, Page M. J. Am. Chem. Soc 1999;121:4720.
11. Quapp W. J. Mol. Struct 2004;695–696:95.
12. Taketsugu T, Tajima N, Hirao K. J. Chem. Phys 1996;105:1933.
13. Miller WH, Handy NC, Adams JE. J. Chem. Phys 1980;72:99.González J, Gliménez X, Bofill JM. J. Chem. Phys 2002;116:8713.
14. Quapp W, Hirsch M, Imig O, Heidrich D. J. Comput. Chem 1998;19:1087.Quapp W, Hirsch M, Heidrich D. Theor. Chem. Acc 1998;1000:285.
15. Quapp W, Hirsch M, Heidrich D. Theor. Chem. Acc 2000;105:145.Quapp W, Hirsch M, Heidrich D. Theor. Chem. Acc 2004;112:40.Quapp W. J. Theor. Comp. Chem 2003;2:385.
16. Jiménez A, Crehuet R. Theor. Chem. Acc 2007;118:769.
17. Williams IH, MAggiora GM. J. Mol. Struct.-THEOCHEM 1982;89:365.
18. Kumeda Y, Taketsugu T. J. Chem. Phys 2000;113:477.
19. Lasorne B, Dive G, Desouter-Lecomte M. J. Chem. Phys 2003;118:5831.
20. Colwell SM. Mol. Phys 1984;51:1217.Colwell SM, Handy NC. J. Chem. Phys 1985;82:1281.Baker J, Gill PMW. J. Comput. Chem 1988;9:465.Yanai T, Taketsugu T, Hirao K. J. Chem. Phys 1997;107:1137.
21. Hrovat DA, Borden WT. J. Am. Chem. Soc 1992;114:5879.
22. Wenthold PG, Hrovat DA, Borden WT, Lineberger WC. Science 1996;272:1456. [PubMed: 8662467]
23. Castaño O, Palmeiro R, Frutos LM, Luisandrés J. J. Comput. Chem 2002;23:732. [PubMed: 11948591]
24. Castaño O, Frutos L-M, Palmeiro R, Notario R, Andrés J-L, Gomperts R, Blancafort L, Robb MA. Angew. Chem. Int. Ed 2000;39:2095.
25. Shapley WA, Bacskay GB. J. Phys. Chem. A 1999;103:6624.
26. Finnerty JJ, Wentrup C. J. Org. Chem 2004;69:1909. [PubMed: 15058936]Finnerty JJ, Wentrup C. J. Org. Chem 2005;70:9735. [PubMed: 16292801]
27. Yamamoto N, Bernardi F, Bottoni A, Olivucci M, Robb MA, Wilsey S. J. Am. Chem. Soc 1994;116:2064.Malone S, Hegarty AF, Nguyen MT. J. Chem. Soc. Perkin Trans 1988;2:477.Tokmakov IV, Kim G-S, Kislov VV, Mebel AM, Lin MC. J. Phys. Chem. A 2005;109:6114. [PubMed: 16833949]
28. Shaik S, Danovich D, Sastry GN, Ayala PY, Schlegel HB. J. Am. Chem. Soc 1997;119:9237.Sastry GN, Shaik S. J. Am. Chem. Soc 1998;120:2131.
29. Li J, Li X, Shaik S, Schlegel HB. J. Phys. Chem. A 2004;108:8526.Bakken V, Danovich D, Shaik S, Schlegel HB. J. Am. Chem. Soc 2001;123:130. [PubMed: 11273609]
30. Yamataka H, Aida M, Dupuis M. Chem. Phys. Lett 1999;300:583.Yamataka H, Aida M, Dupuis M. Chem. Phys. Lett 2002;353:310.
31. Valtazanos P, Elbert ST, Xantheas S, Ruedenberg K. Theor. Chem. Acc 1991;78:287.Xantheas S, Elbert ST, Ruedenberg K. Theor. Chim. Acta 1991;78:327.Xantheas S, Elbert ST, Ruedenberg K. Theor. Chim. Acta 1991;78:365.Valtazanos P, Ruedenberg K. Theor. Chim. Acta 1991;78:397.Valtazanos P, Elbert ST, Ruedenberg K. J. Am. Chem. Soc 1986;108:3147.Kraus WA, DePristo AE. Theor. Chim. Acta 1986;69:309.
32. Nouri DH, Tantillo DJ. J. Org. Chem 2006;71:3686. [PubMed: 16674038]
33. Bartsch RA, Chae YM, Ham S, Birney DM. J. Am. Chem. Soc 2001;123:7479. [PubMed: 11480966]
34. Hrovat DA, Duncan JA, Borden WT. J. Am. Chem. Soc 1999;121:169.
35. Roth WR, Wollweber D, Offerhas R, Rekowski V, Lennartz HW, Sustmann R, Müller W. Chem. Ber 1993;126:2701.

36. Debbert SL, Carpenter BK, Hrovat DA, Borden WT. J. Am. Chem. Soc 2002;124:7896. [PubMed: 12095322]
37. Suhrada CP, Selçuki C, Nendel M, Cannizzaro C, Houk KN, Rissing P-J, Baumann D, Hasselmann D. Angew. Chem. Int. Ed 2005;44:3548.
38. Reyes MB, Lobkovsky EB, Carpenter BK. J. Am. Chem. Soc 2002;102:641. [PubMed: 11804495]
39. Özkan I, Zora M. J. Org. Chem 2003;68:9635. [PubMed: 14656088]
40. Stephenson LM, Grdina MJ, Orfanopoulos M. Acc. Chem. Res 1980;13:419.
41. Yamaguchi K, Yabushita S, Fueno T, Houk KN. J. Am. Chem. Soc 1981;103:5043.Tonachini G, Schlegel HB, Bernardi F, Robb MA. J. Am. Chem. Soc 1990;112:483.
42. Orfanopoulos M, Stephenson LM. J. Am. Chem. Soc 1980;102:1417.Grdina MB, Orfanopoulos M, Stephenson LM. J. Am. Chem. Soc 1979;101:3111.
43. Leach AG, Houk KN. Chem. Commun 2002;2002:1243.
44. Singleton DA, Hang C, Symanski MJ, Greenwald EE. J. Am. Chem. Soc 2003;125:1176. [PubMed: 12553813]
45. González-Lafont À, Moreno M, Lluch JM. J. Am. Chem. Soc 2004;126:13089. [PubMed: 15469307]
46. Wenthold PG, Lipton MA. J. Am. Chem. Soc 2000;122:9265.
47. Bekele T, Christian CF, Lipton MA, Singleton DA. J. Am. Chem. Soc 2005;127:9216. [PubMed: 15969600]
48. Schmittel M, Vavilala C, Jaquet R. Angew. Chem. Int. Ed 2007;46:6911.
49. Sakai S, Nguyen MT. J. Phys. Chem. A 2000;104:9169.
50. Kraka E, Wu A, Cremer D. J. Phys. Chem. A 2003;107:9008.
51. Toma L, Romano S, Quadrelli P, Caramella P. Tet. Lett 2001;42:5077.
52. Caramella P, Quadrelli P, Toma L. J. Am. Chem. Soc 2002;124:1130. [PubMed: 11841256]
53. Quadrelli P, Romano S, Toma L, Caramella P. Tet. Lett 2002;43:8785.
54. Quadrelli P, Romano S, Toma L, Caramella P. J. Org. Chem 2003;68:6035. [PubMed: 12868944]
55. Dinadayalane TC, Sastry GN. Organometallics 2003;22:5526.Dinadayalane TC, Gayatri G, Sastry GN, Leszczynski J. J. Phys. Chem. A 2005;109:9310. [PubMed: 16833273]
56. Lasorne B, Dive G, Desouter-Lecomte M. J. Chem. Phys 2005;122:184304. [PubMed: 15918701]
57. Limanto J, Khuong KS, Houk KN, Snapper ML. J. Am. Chem. Soc 2003;125:16310. [PubMed: 14692772]
58. Çelebi-Ölçüm N, Ess DH, Aviyente V, Houk KN. J. Am. Chem. Soc 2007;129:4528. [PubMed: 17385868]
59. Ussing BR, Hang C, Singleton DA. J. Am. Chem. Soc 2006;128:7594. [PubMed: 16756316]
60. Gagnepain J, Castet F, Quideau S. Angew. Chem. Int. Ed 2007;46:1533.Gagnepain J, Méreau R, Dejugnac D, Léger J-M, Castet F, Deffieux D, Pouységu L, Quideau S. Tetrahedron 2007;63:6493.
61. Leach AG, Goldstein E, Houk KN. J. Am. Chem. Soc 2003;125:8330. [PubMed: 12837105]
62. Mawhinney RC, Muchall HM, Peslherbe GH. Can. J. Chem 2005;83:1615.
63. Merrer DC, Rablen PR. J. Org. Chem 2005;70:1630. [PubMed: 15730281]Khrapunovich M, Zelenova E, Seu L, Sabo AN, Flaherty A, Merrer DC. J. Org. Chem 2007;72:7574. [PubMed: 17824649]
64. Zhou C, Birney DM. Org. Lett 2002;4:3279. [PubMed: 12227768]Bettinger HF, Kaiser RI. J. Phys. Chem. A 2004;108:4576.Chen L, Xiao H, Xiao J, Gong X. J. Phys. Chem. A 2003;107:11440.

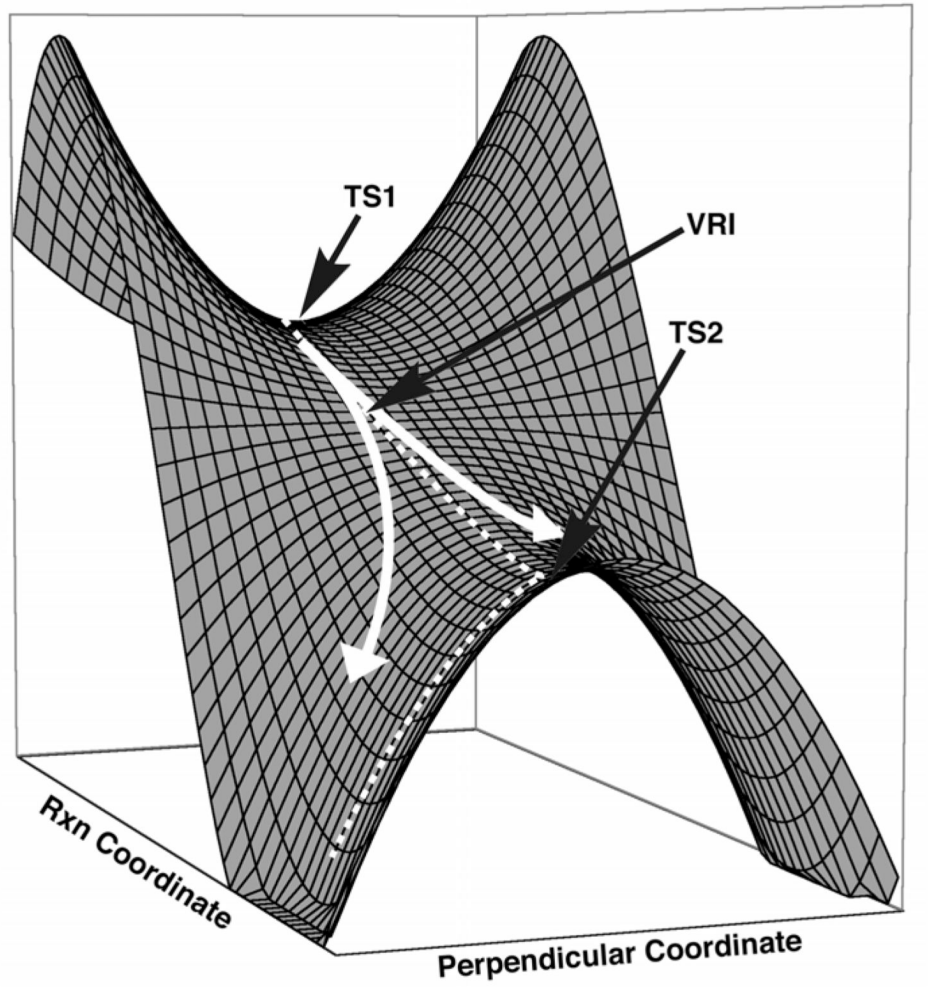

Figure 1.
Model potential energy surface with sequential transition states. Dotted white lines represent the IRC pathway while solid lines represent expected reaction trajectories.

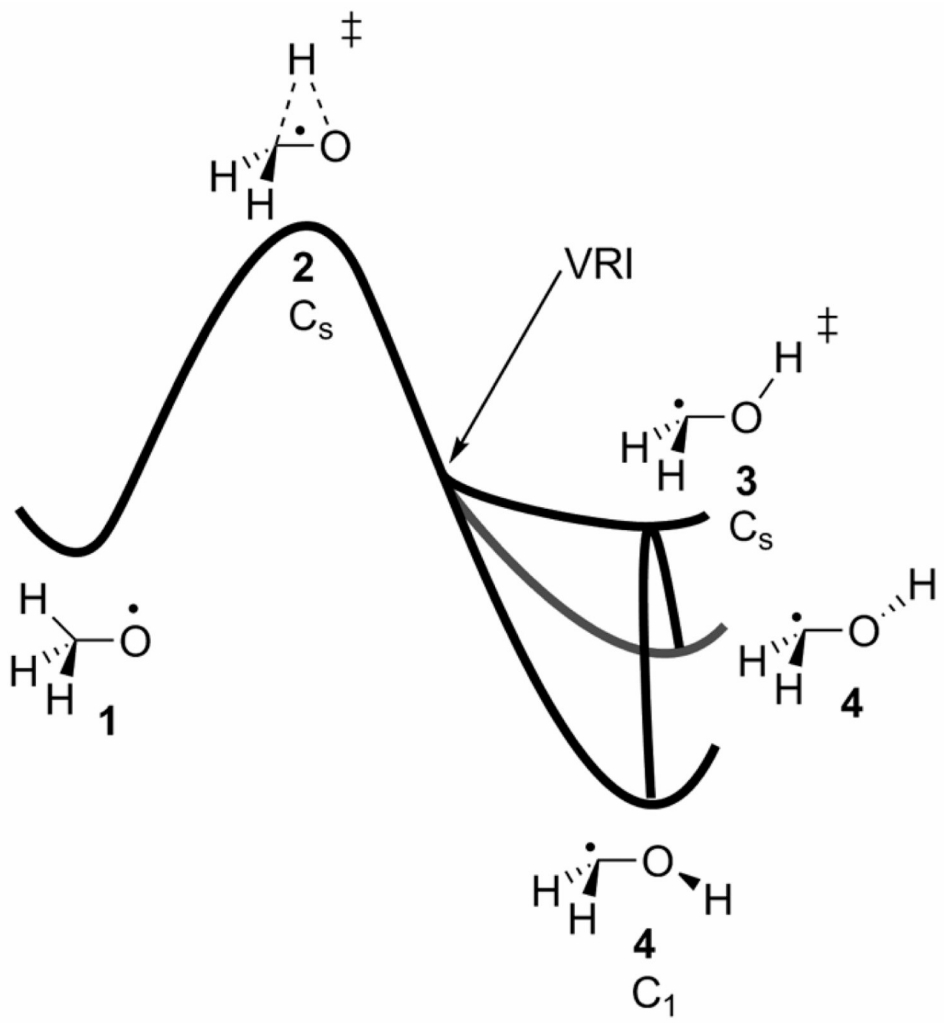

Figure 2.
Isomerization of methoxy radical to hydroxymethylene radical.

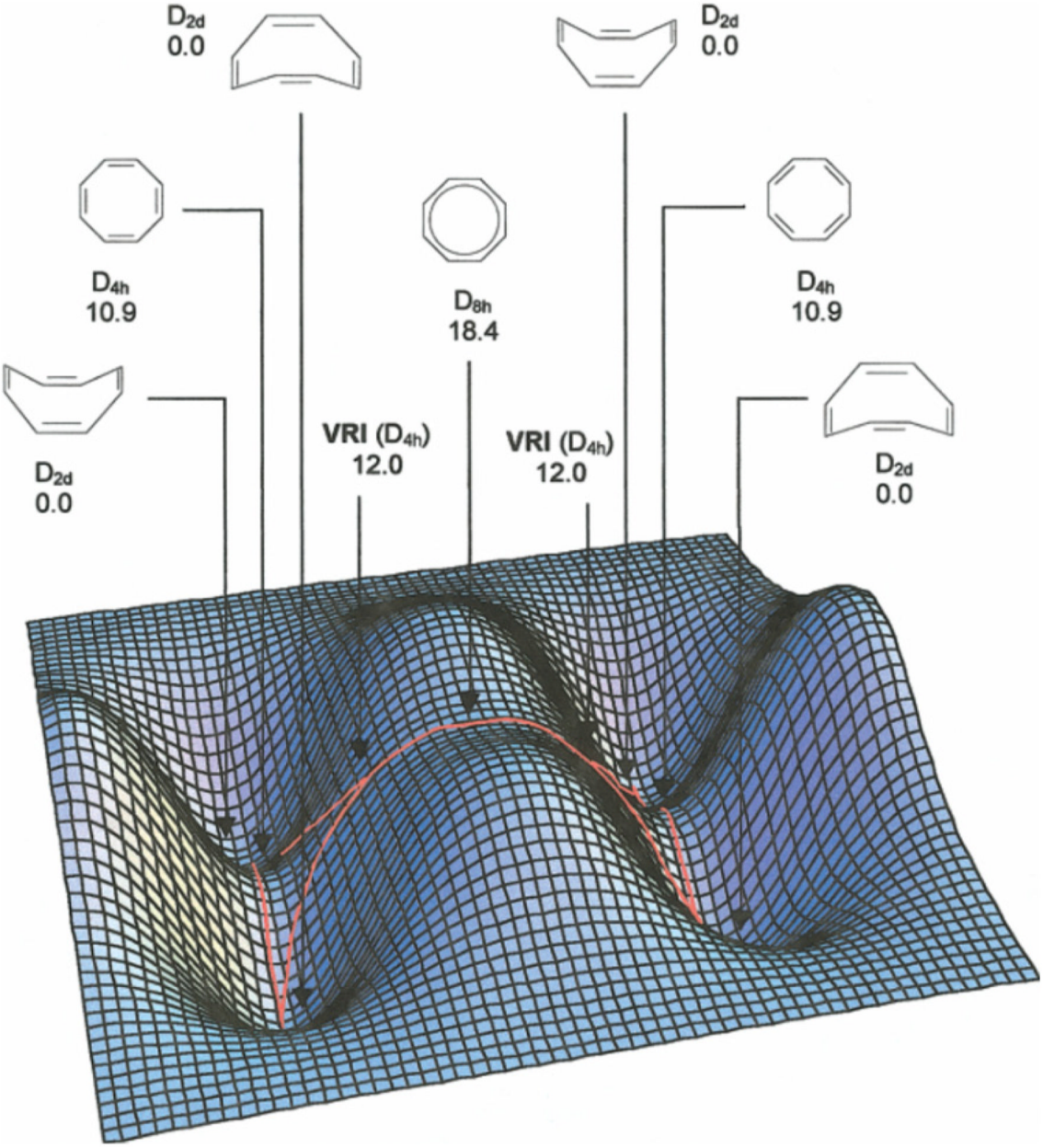

Figure 3.
CASSCF/6-31G* potential energy surface for the bond shifting of cyclooctatetraene. Reprinted with permission from reference [23]. Copyright Wiley 2002.

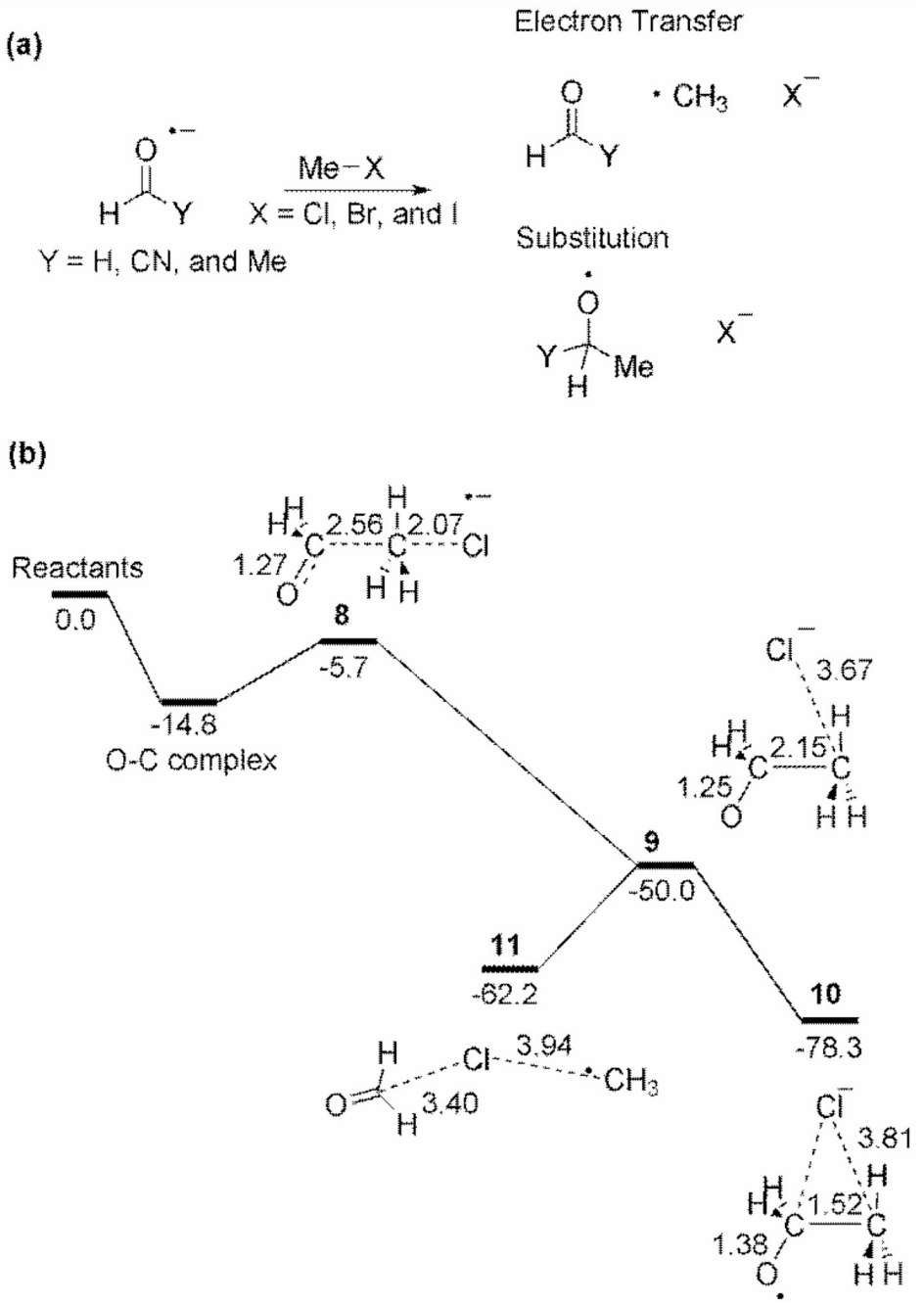

Figure 4.

(a) Substitution and electron transfer reactions for aldehyde anion radical additions to alkyl halides. (b) (U)QCISD(T) PES for the reaction of aldehyde anion radical with methylchloride. IRC starting at **8** leads to **10**, while the reaction path in non-mass-weighted coordinates leads from **8** to **11**. Energies and geometries taken from reference [28].

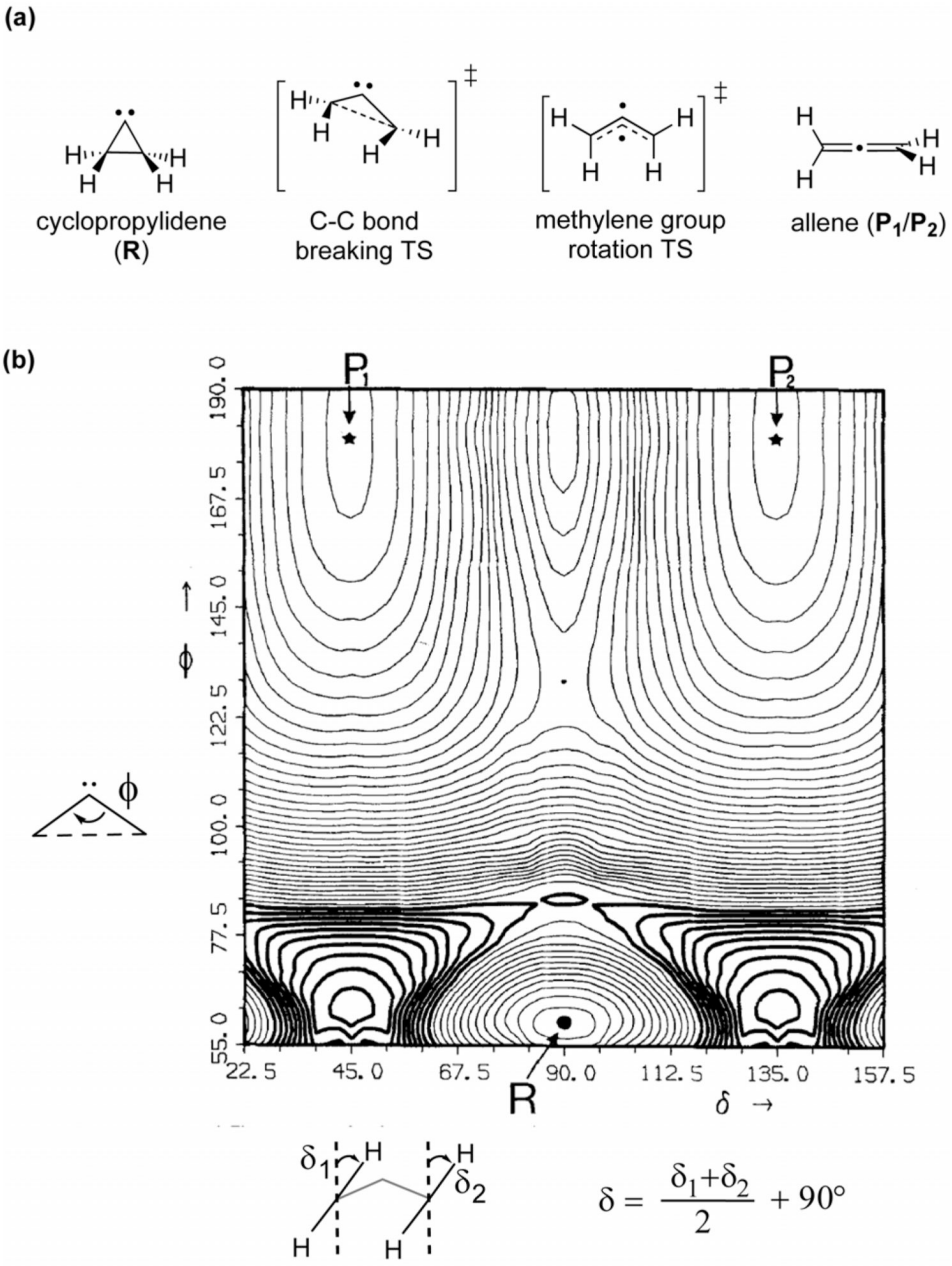

Figure 5.

(a) Cyclopropylidene (**R**) to allene (**P**$_1$/**P**$_2$) rearrangement stationary points. (b) MCSCF potential energy surface. Reprinted with permission from reference [2] Copyright Springer 1986.

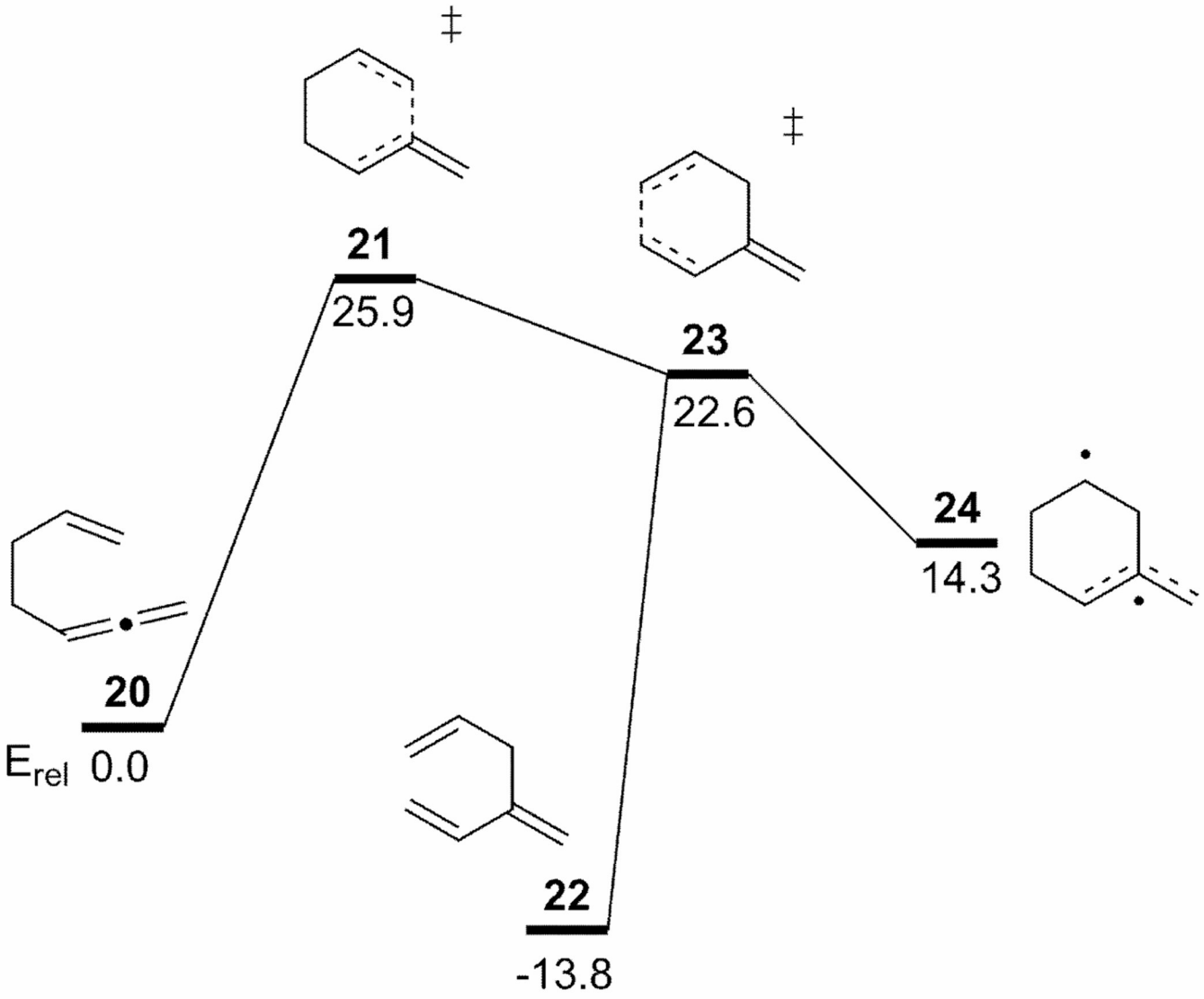

Figure 6.
PES for the rearrangement of 1,2,6-heptatriene to 1,3,6-heptatriene. IRC calculations using DFT lead from **21** to **22**, while the IRC computed using CASSCF connects **21** to **24**. CASPT2 (8,8)/6-31G* energies (kcal/mol) taken from reference [34].

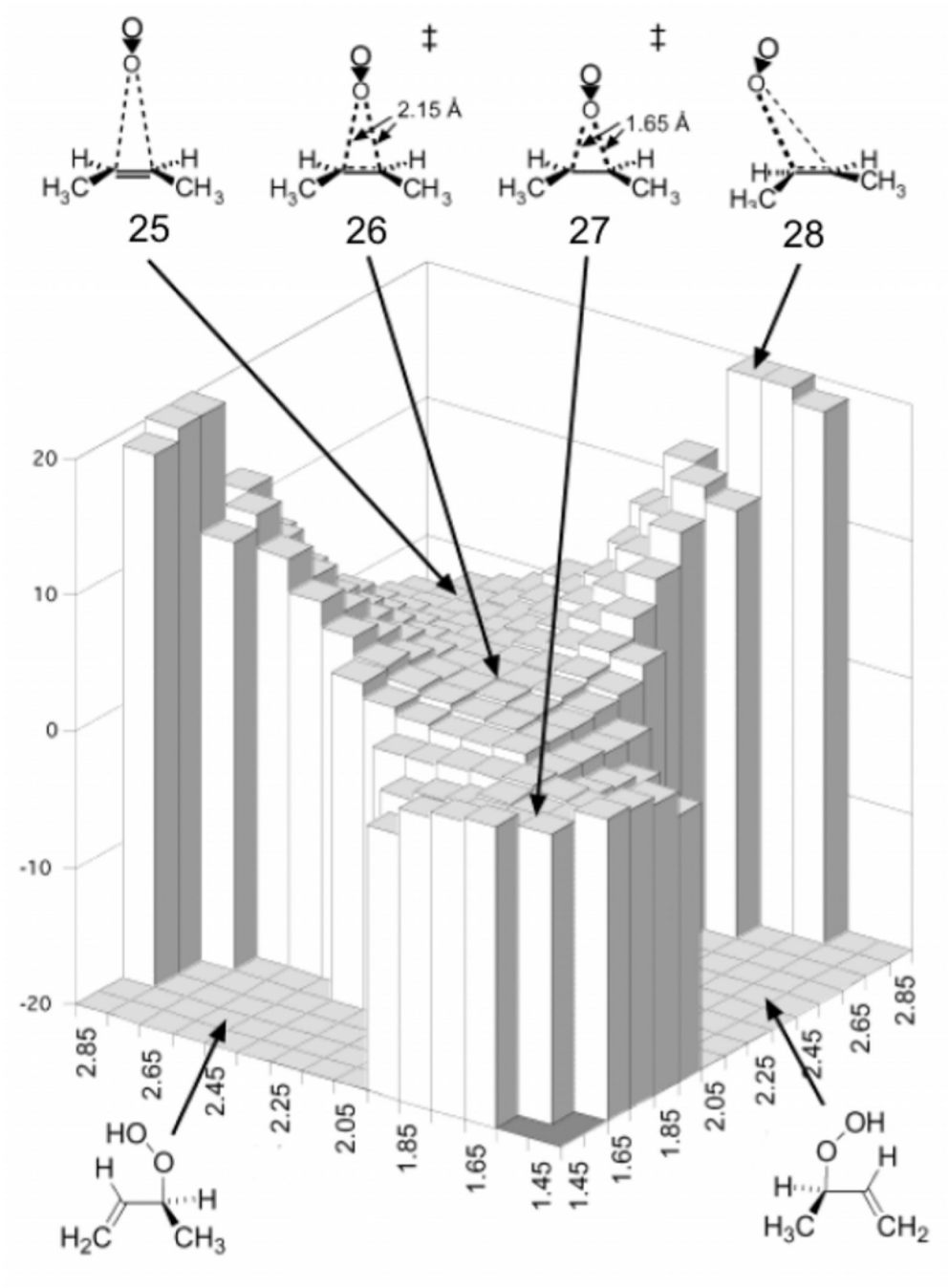

Figure 7.
CCSD(T)//B3LYP potential energy surface of the singlet O_2 ene reaction mapped according to the average alkene C-O distances. Adapted with permission from reference [3]. Copyright 2003 American Chemical Society.

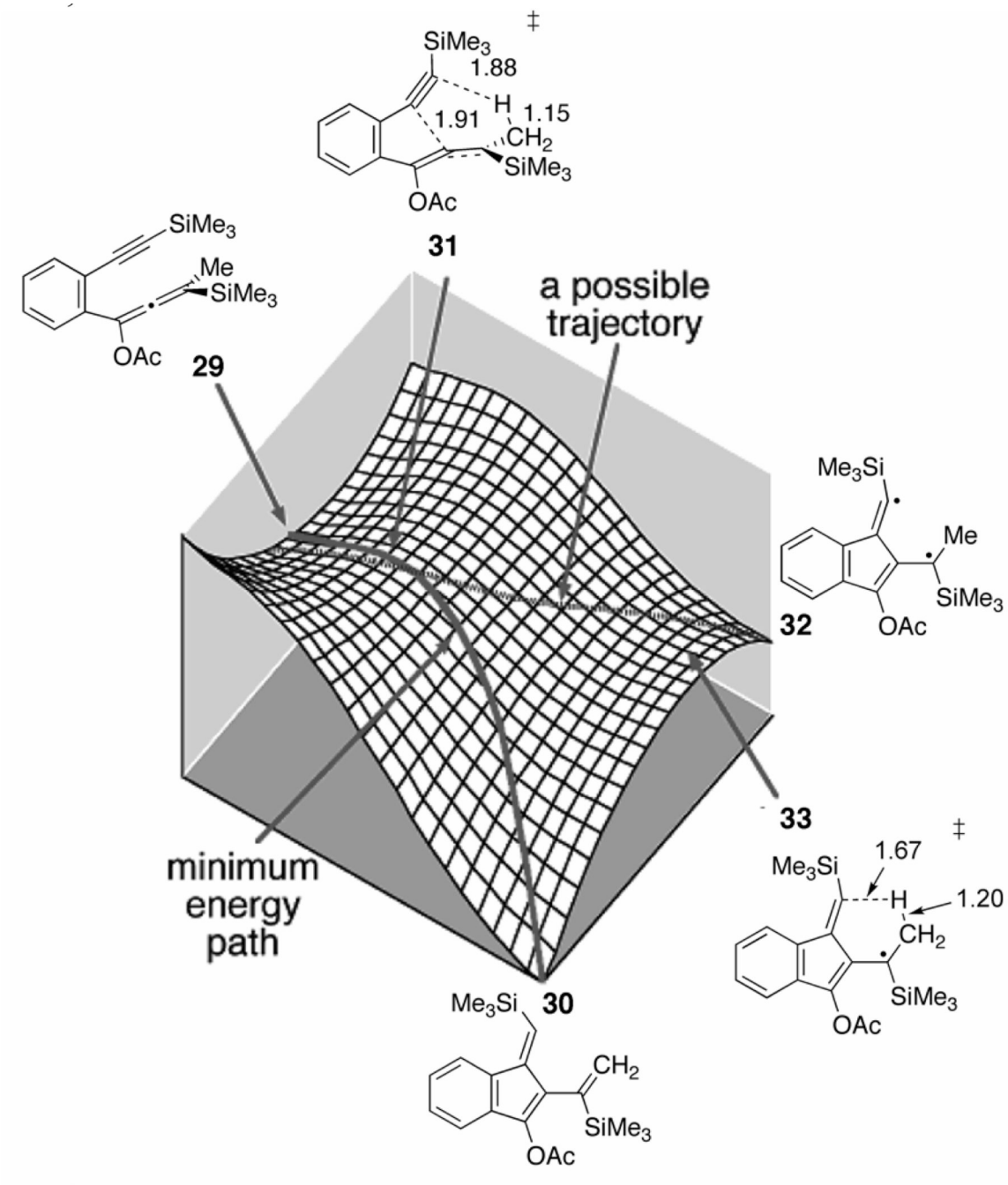

Figure 8.

Qualitative unsymmetrical bifurcating PES for the oxyanion substituted C^2-C^6 cyclization (UB3LYP/6-31G** TS geometries). Adapted with permission from reference [47]. Copyright 2005 American Chemical Society.

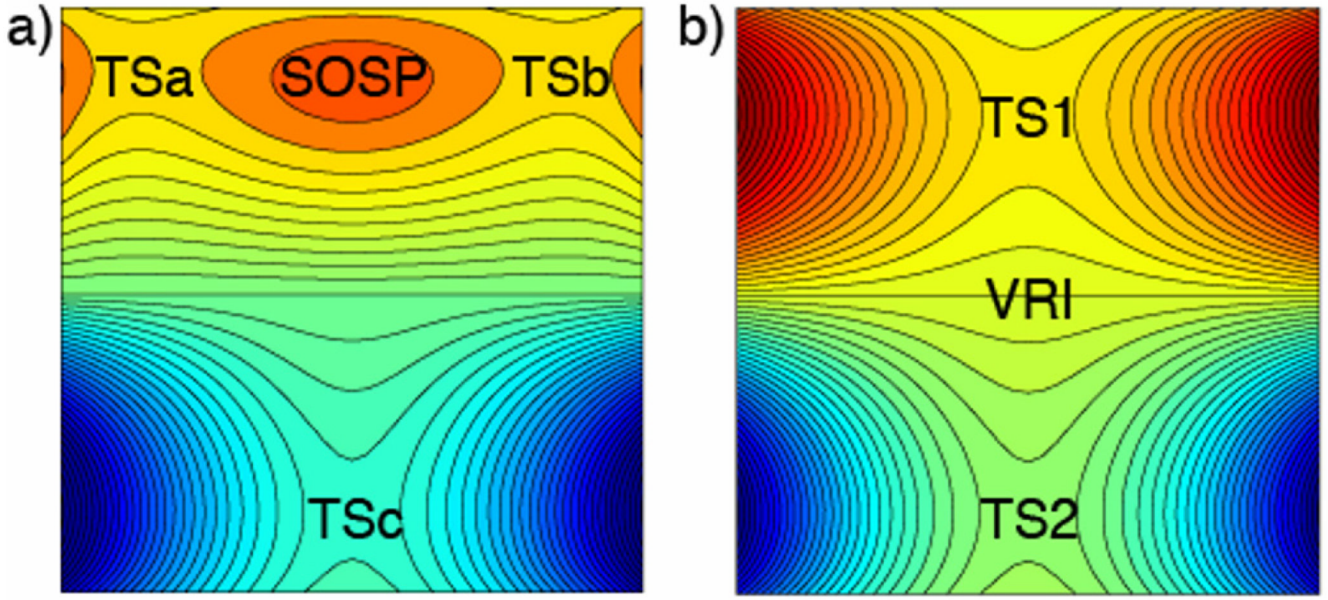

Figure 9.
Model potential energy surface contour plots for (a) pericyclic and (b) bis-pericyclic cycloaddition. [High E = Red, Low E = Blue]

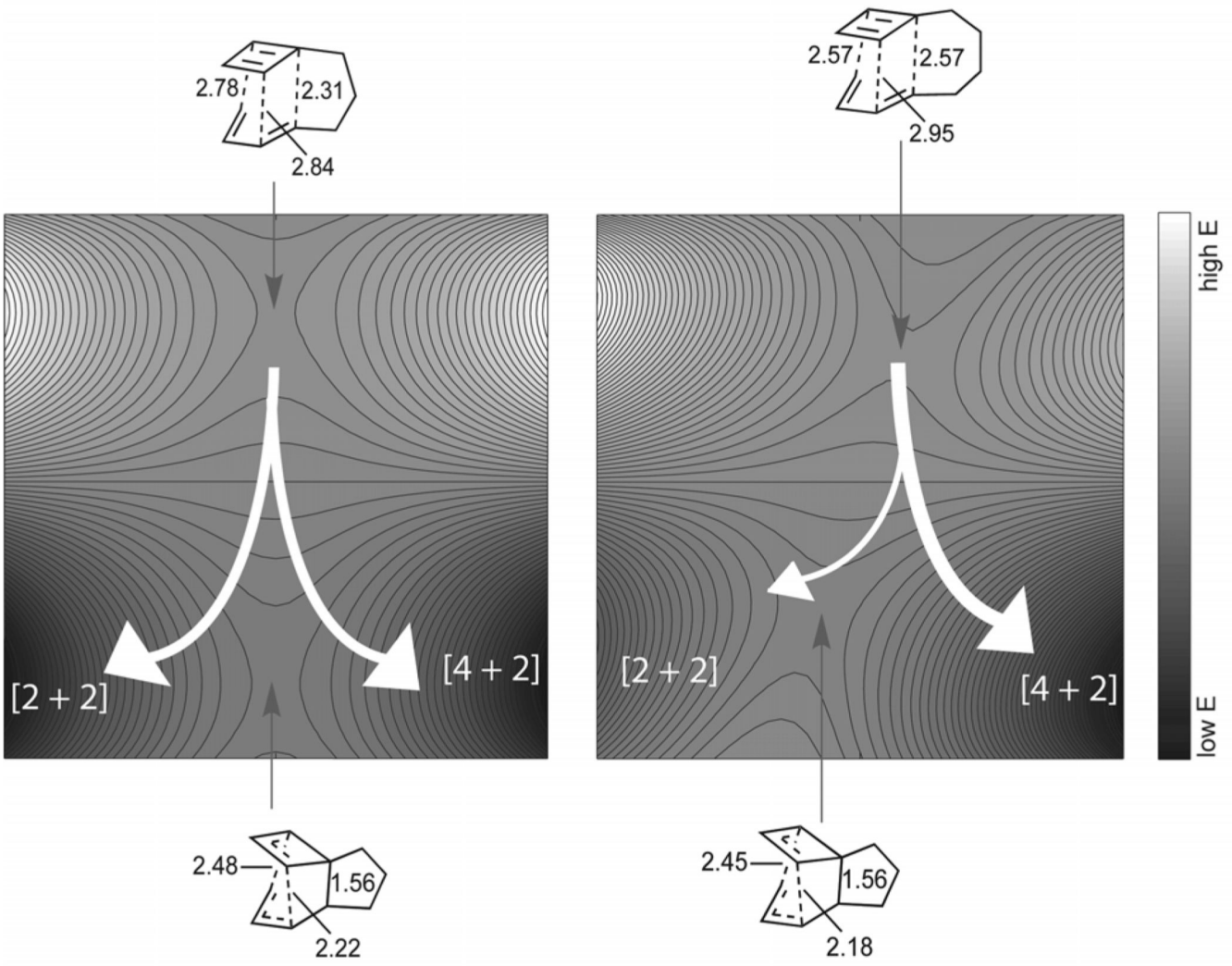

Figure 10.
Qualitative PESs for cycloaddition of cyclobutadiene and butadiene with trimethylene and tetramethylene tethers. Energies and geometries taken from reference [57].

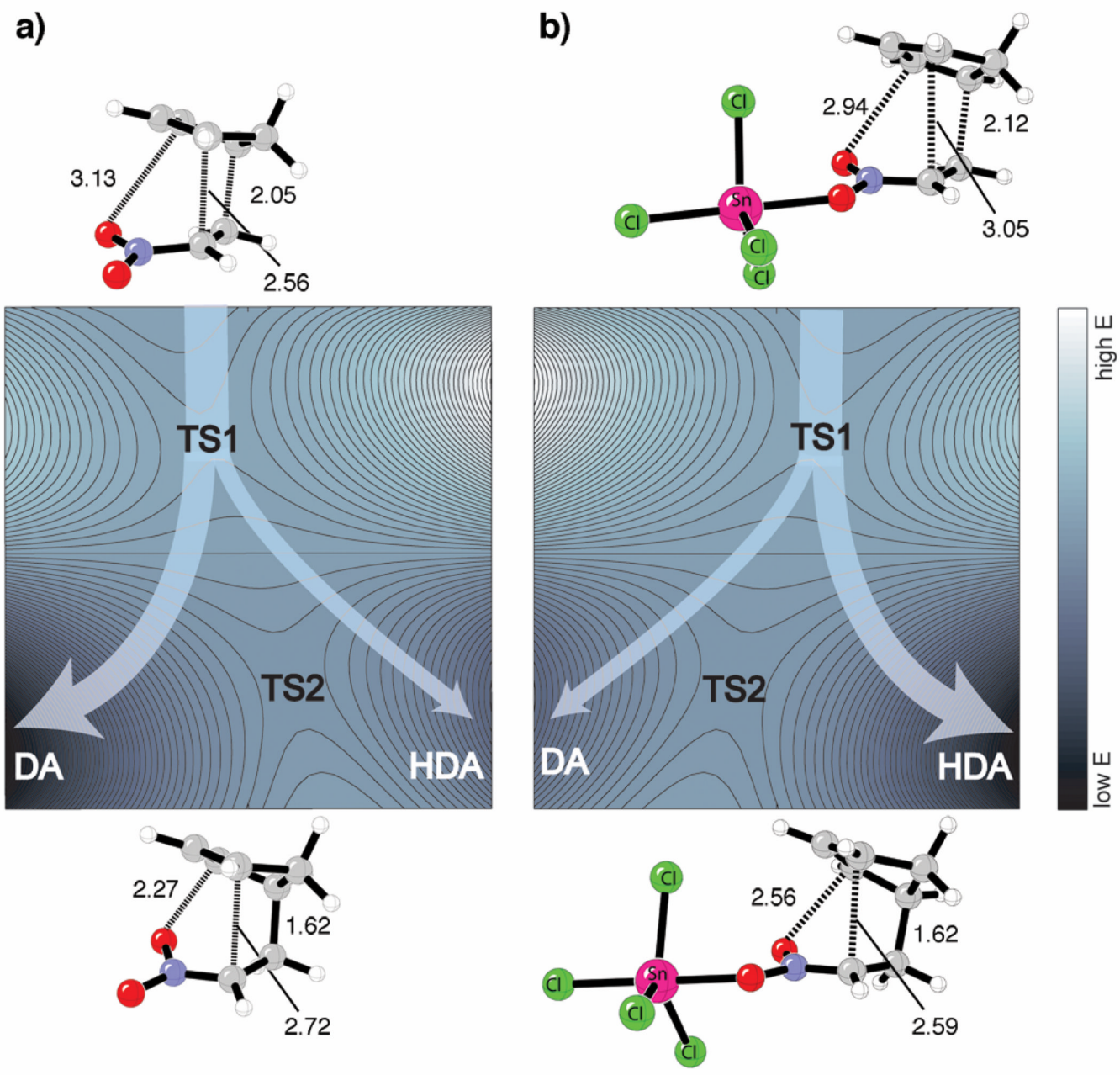

Figure 11.
Qualitative contour plots and transition state structures for (a) thermal and (b) Lewis-acid catalyzed Diels-Alder cycloaddition of cyclopentadiene with nitroethylene. Adapted with permission from reference [58]. Copyright 2007 American Chemical Society.

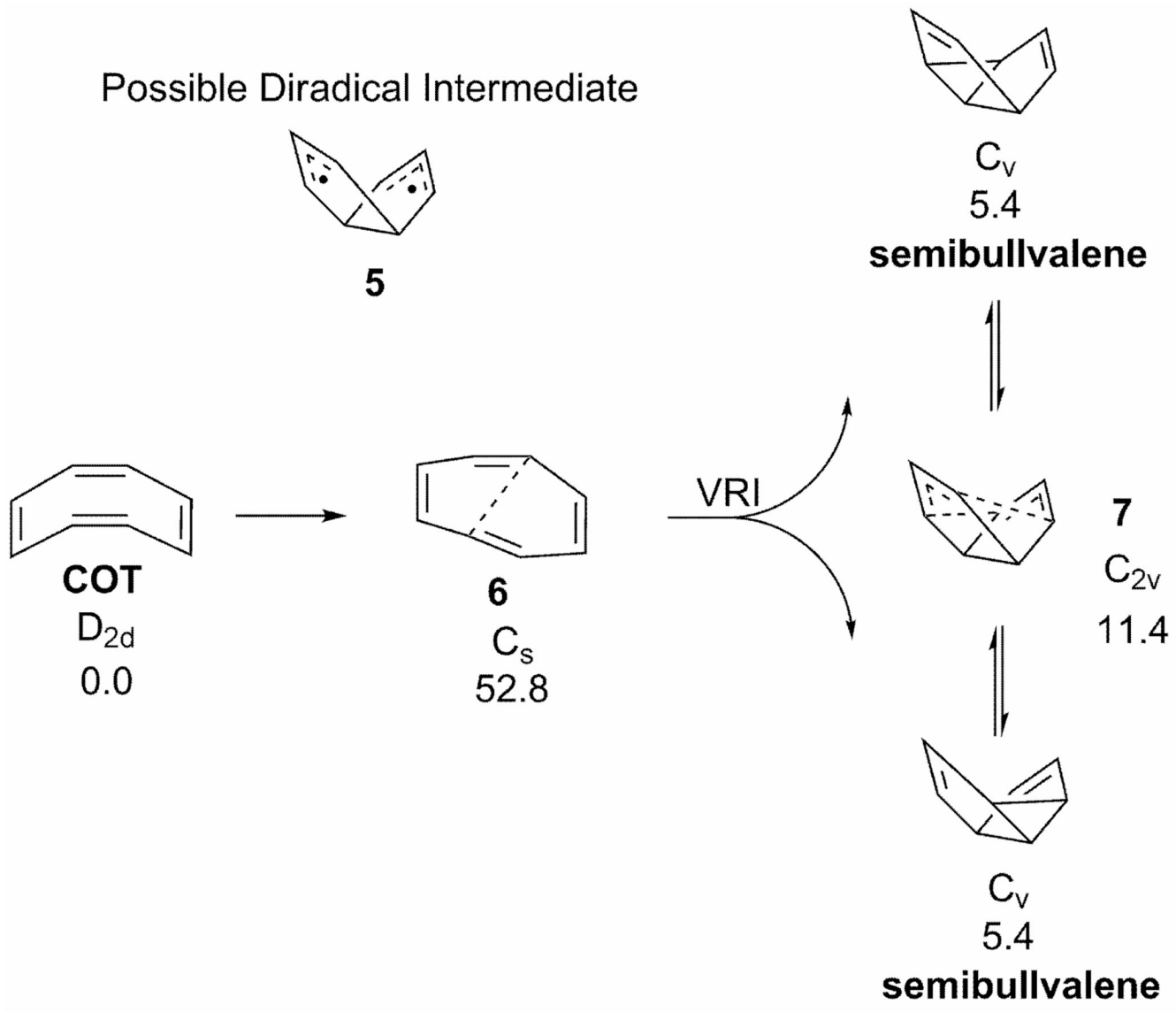

Scheme 1.
Stationary points along the CAS(MP2)/CASSCF potential energy surface for the transformation of COT to semibullvalene. Energies taken from reference [24] (kcal/mol).

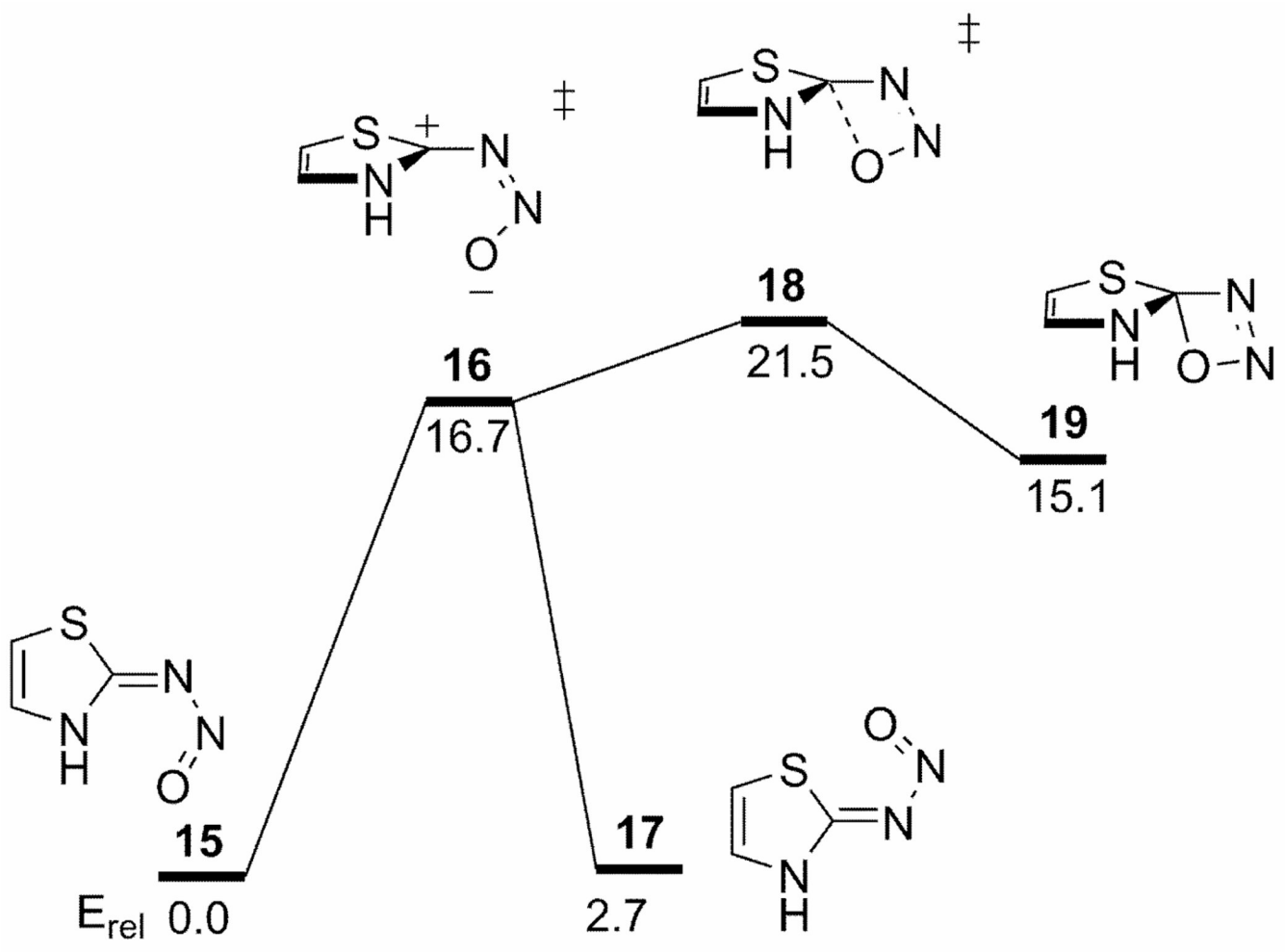

Scheme 2.
MP4SDQ stationary points for the thermal deazetization of heterocyclic nitrosimines. Energies taken from reference [33] (kcal/mol).

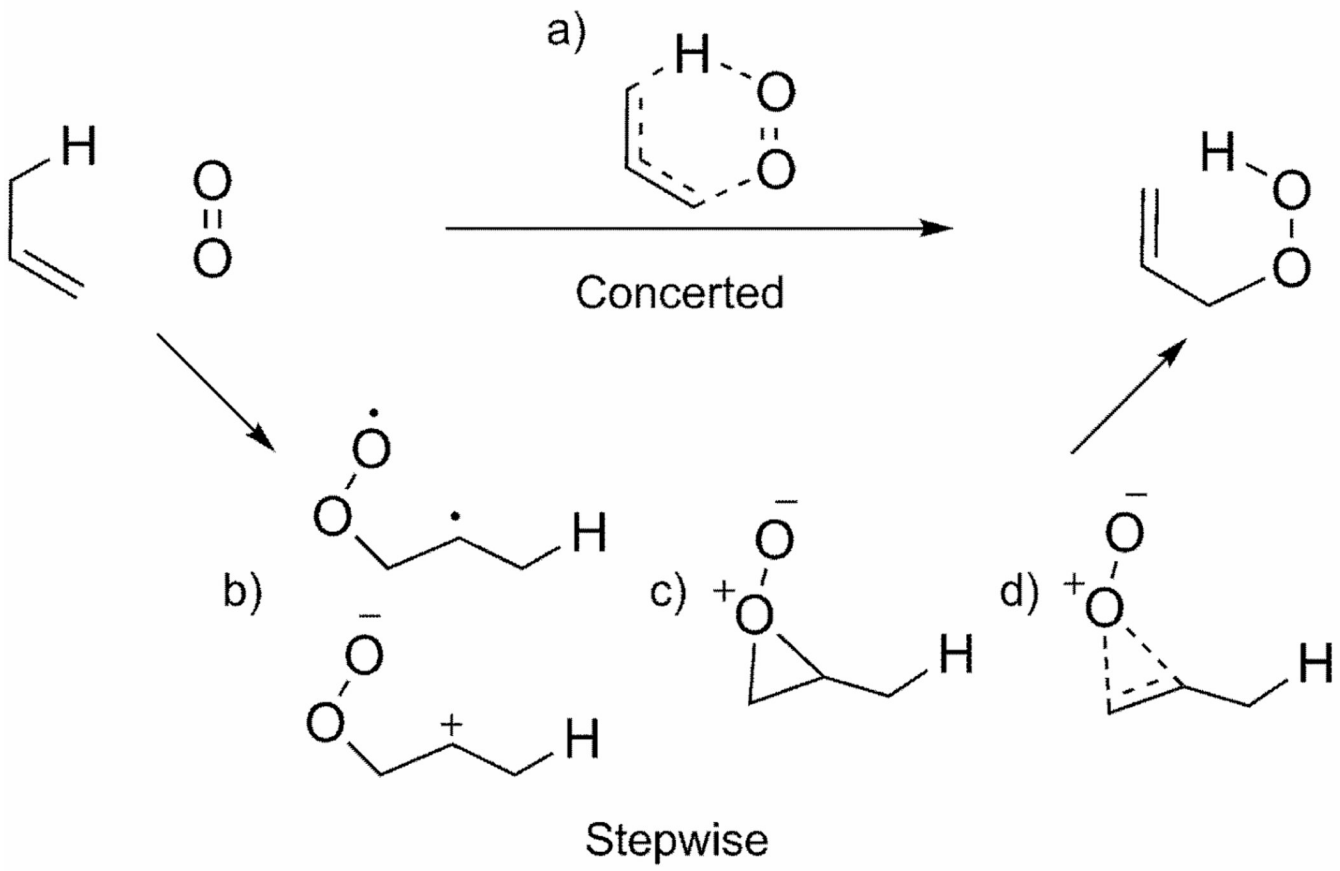

Scheme 3.
Concerted and stepwise mechanisms for the singlet oxygen ene reaction. Structures b–d represent possible intermediates.

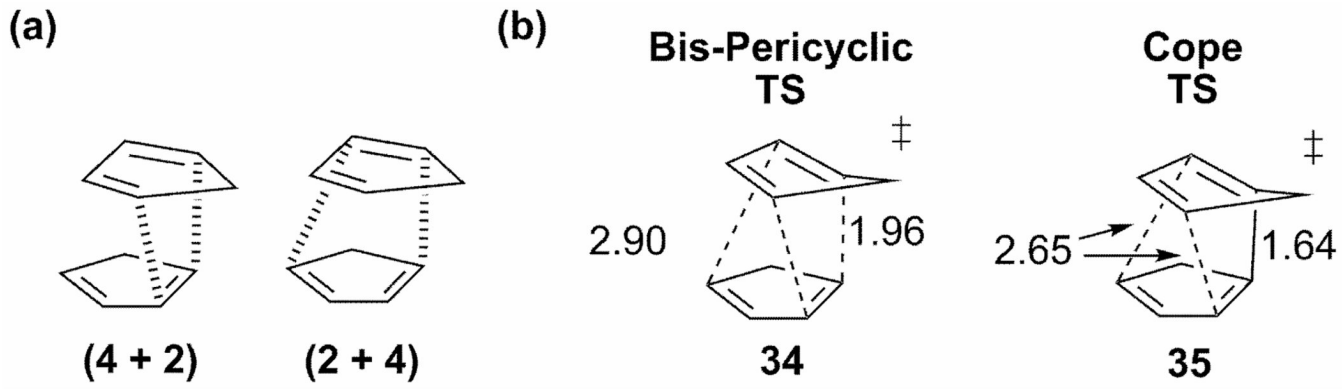

Scheme 4.
Endo cyclopentadiene dimerization (a) [4 + 2] interactions; (b) TS structures from reference [52].

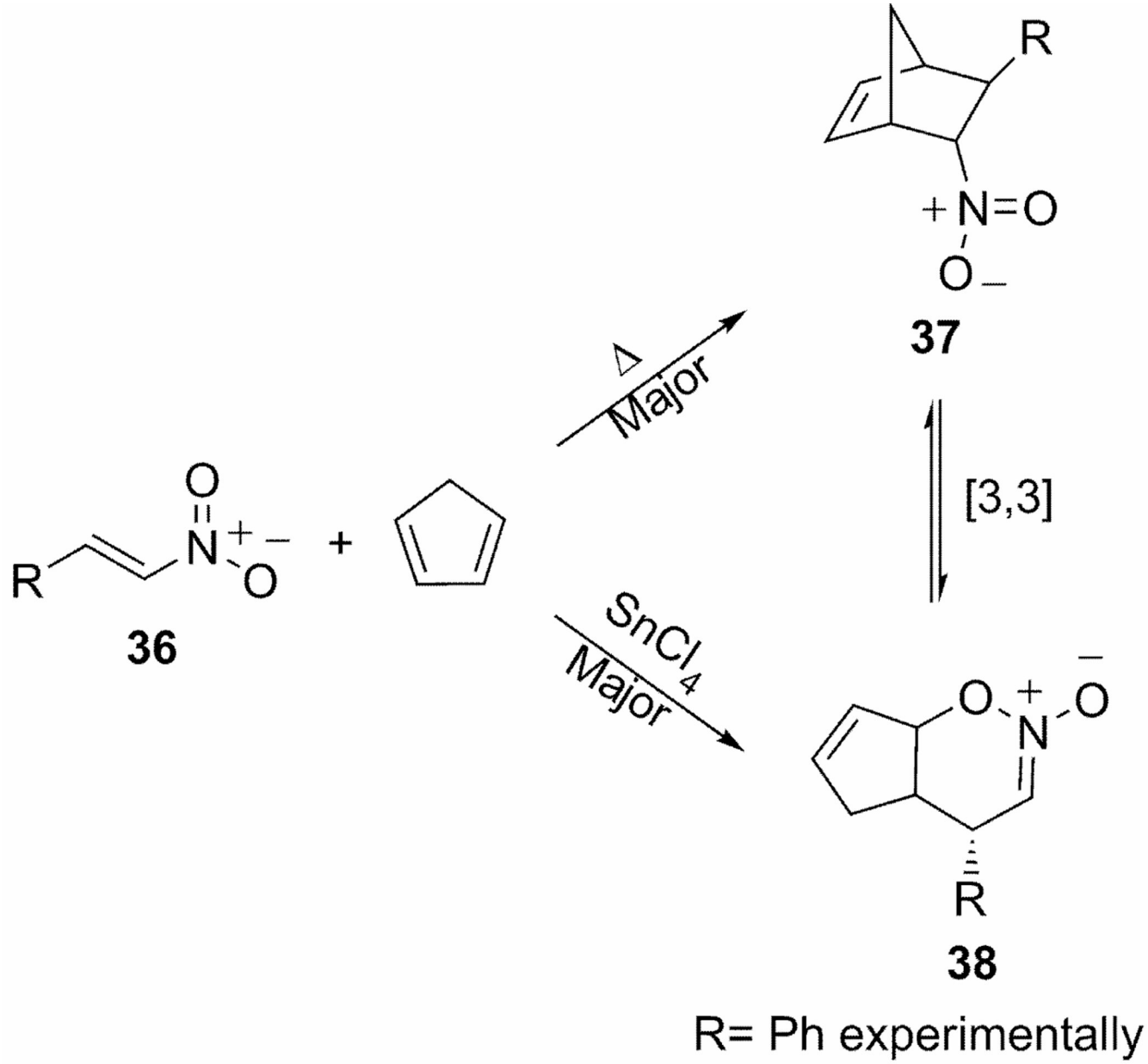

Scheme 5.
Competing Diels-Alder and hetero-Diels-Alder cycloadditions for cyclopentadiene addition to nitroethylene.